REPORT

# A Mutation in the Golgi Qb-SNARE Gene *GOSR2* Causes Progressive Myoclonus Epilepsy with Early Ataxia

Mark A. Corbett,[1,17] Michael Schwake,[2,17] Melanie Bahlo,[3,4] Leanne M. Dibbens,[1,5] Meng Lin,[2] Luke C. Gandolfo,[3] Danya F. Vears,[6] John D. O'Sullivan,[7] Thomas Robertson,[8] Marta A. Bayly,[1] Alison E. Gardner,[9] Annemarie M. Vlaar,[10] G. Christoph Korenke,[11] Bastiaan R. Bloem,[12] Irenaeus F. de Coo,[13] Judith M.A. Verhagen,[14] Anna-Elina Lehesjoki,[15] Jozef Gecz,[1,5,9,16,*] and Samuel F. Berkovic[6,*]

The progressive myoclonus epilepsies (PMEs) are a group of predominantly recessive disorders that present with action myoclonus, tonic-clonic seizures, and progressive neurological decline. Many PMEs have similar clinical presentations yet are genetically heterogeneous, making accurate diagnosis difficult. A locus for PME was mapped in a consanguineous family with a single affected individual to chromosome 17q21. An identical-by-descent, homozygous mutation in *GOSR2* (c.430G>T, p.Gly144Trp), a Golgi vesicle transport gene, was identified in this patient and in four apparently unrelated individuals. A comparison of the phenotypes in these patients defined a clinically distinct PME syndrome characterized by early-onset ataxia, action myoclonus by age 6, scoliosis, and mildly elevated serum creatine kinase. This p.Gly144Trp mutation is equivalent to a loss of function and results in failure of GOSR2 protein to localize to the *cis*-Golgi.

Clinically, the progressive myoclonus epilepsies (PMEs) can be usefully divided into two groups: those with an associated prominent dementia (e.g., Lafora disease [MIM 254780] and neuronal ceroid lipofuscinoses[1]) and those in which cognition is essentially preserved.[2,3] The paradigmatic form of the latter group is Unverricht-Lundborg disease (ULD; MIM: 254800), which is caused by mutations in *CSTB* (MIM 601145).[4] However, there remains an important group of cases that have a presentation resembling ULD but are not explained by mutations in *CSTB* or other known causes (e.g., mitochondrial disease). Mutations in *SCARB2* (MIM 602257) and *PRICKLE1* (MIM 608500) have been described recently in such families, but most cases remain unsolved.[5–7] We studied one such case in which the clinical onset was marked by ataxia followed by a classic PME presentation without dementia.

The proband (case 1, II-1, Australian pedigree, Figure 1B) was Australian, born to second-cousin parents of British origin. When she was 2 years old, she was observed to have difficulty walking. The patient was found to be areflexic, but development was otherwise normal. At age 7, she had a tremor, and subsequently it became clear that action myoclonus and occasional absence seizures were present. At age 13, she began having drop attacks as well as major convulsive seizures. She required a wheelchair from age 14 on because of falling attacks and was unable to walk unaided from age 16 on. She had a severe scoliosis requiring surgical correction. By age 22 she was bedfast, and she died at age 32 because of complications from uncontrolled myoclonus. Her intellect was preserved until the last few years of her life, when there was mild cognitive impairment. The EEG showed active generalized spike and wave discharges, which worsened with intermittent photic stimulation. Her MRI and nerve conduction studies were normal. A complete autopsy was performed. The immediate cause of death was determined to be aspiration bronchopneumonia. The brain showed mild cerebral atrophy and a relatively reduced whole-brain weight of 1129 g, as opposed to a cerebellum weight of 138 g. No gross structural abnormalities were identified at brain dissection. Histologic examination revealed subtle, Alzheimer type II gliosis in the basal ganglia region, consistent with metabolic derangement related to her agonal state. There was minor loss of Purkinje cell and gliosis in the cerebellar vermis but no other focal neuronal degeneration. No abnormal storage material or Lafora bodies were found with examination by

[1]Genetics and Molecular Pathology, SA Pathology, Adelaide 5000, Australia; [2]Department of Biochemistry, Universität Kiel, Kiel D-24098, Germany; [3]The Walter and Eliza Hall Research Institute of Medical Research, Melbourne 3052, Australia; [4]Department of Mathematics and Statistics, University of Melbourne, Parkville 3010, Australia; [5]School of Paediatrics and Reproductive Health, University of Adelaide, Adelaide 5000, Australia; [6]Epilepsy Research Centre, University of Melbourne, Austin Health, West Heidelberg 3084, Australia; [7]Royal Brisbane Clinical School, School of Medicine, University of Queensland, Herston 4006, Australia; [8]Anatomical Pathology, Pathology Queensland, Royal Brisbane and Women's, Herston 4029, Australia; [9]Women's and Children's Health Research Institute, North Adelaide 5006, Australia; [10]Department of Neurology, St. Lucas Andreas Ziekenhuis, Amsterdam 1061 AE, The Netherlands; [11]Department of Neuropediatrics, Klinikum Oldenburg, Oldenburg D-26131, Germany; [12]Department of Neurology, Donders Institute for Brain, Cognition and Behaviour, Radboud University Nijmegen Medical Center, Nijmegen 6500 HB, The Netherlands; [13]Department of Neurology, Erasmus MC, Rotterdam 3015 CE, The Netherlands; [14]Department of Clinical Genetics, Erasmus MC, Rotterdam 3015 CE, The Netherlands; [15]Folkhälsan Institute of Genetics, Department of Medical Genetics and Neuroscience Center, University of Helsinki 00014, Finland; [16]School of Molecular and Biomedical Sciences, University of Adelaide, Adelaide 5000, Australia
[17]These authors contributed equally to this work
*Correspondence: jozef.gecz@adelaide.edu.au (J.G.), samuelfb@unimelb.edu.au (S.F.B.)
DOI 10.1016/j.ajhg.2011.04.011. 

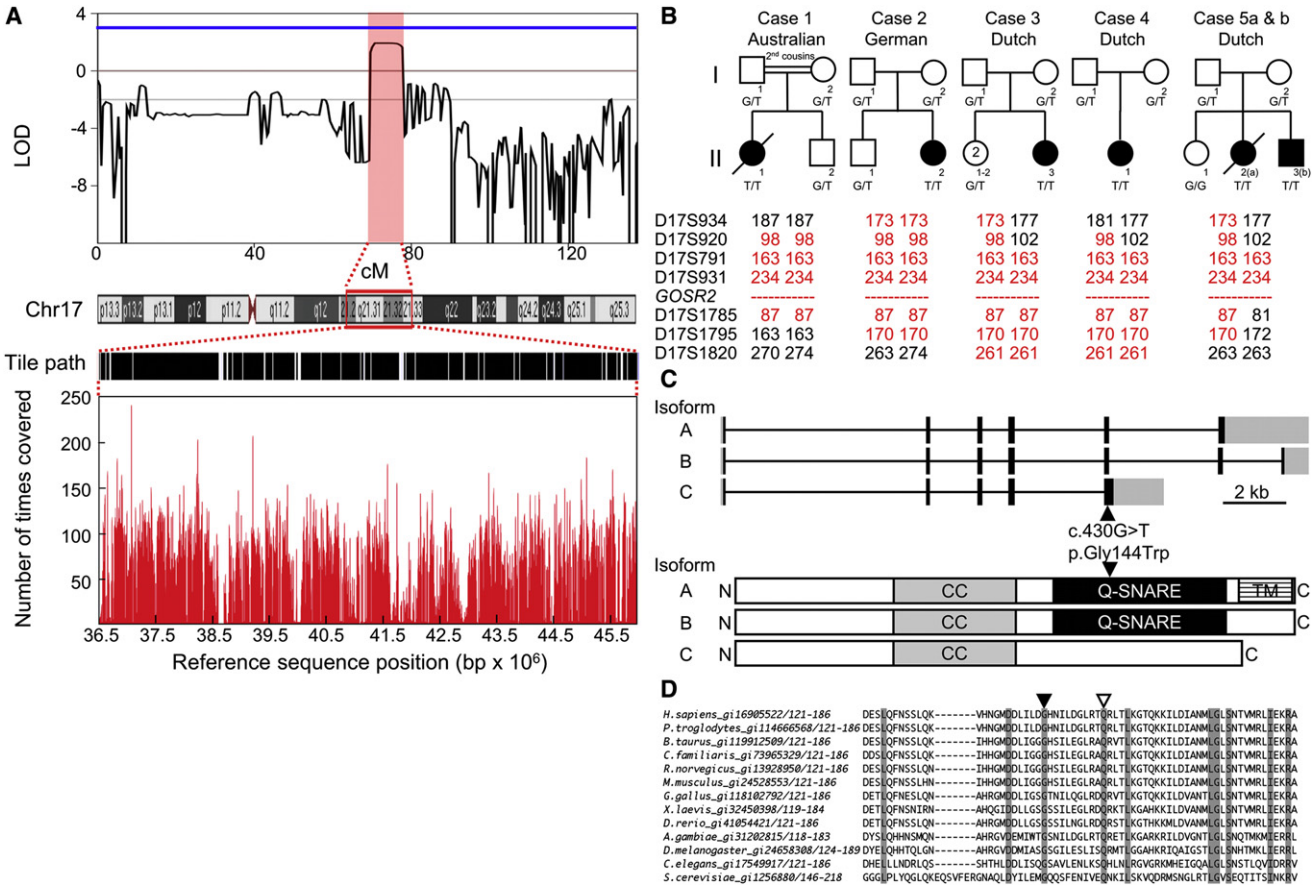


**Figure 1. Identification of *GOSR2* Mutation**

(A) Graph showing the computed LOD scores for chromosome 17. A single peak, of width 9 cM, with the maximum possible LOD score of 1.93 (indicated by the red highlighting) suggests linkage to a 9.5 Mbp region on chromosome 17 (indicated by the red box on the ideogram). The tile path of regions targeted on the array is indicated by the black shaded regions below the ideogram of chromosome 17. Sequence coverage, calculated as the number of reads per bp of the linkage interval, is indicated in red in the lower graph.

(B) Pedigrees of five families with affected females and males (indicated by black circles and squares, respectively). Alleles carried by each individual are indicated; only affected individuals are homozygous for the *GOSR2* c.430G>T mutation. Below the pedigrees are sizes of products in bp generated by amplification by PCR of microsatellite markers flanking *GOSR2* (indicated on the left) for each affected individual. The red lettering indicates haplotypes observed in more than one individual.

(C) The three isoforms of *GOSR2* (A, B, and C) are shown by exon structure in the context of genomic DNA (upper half) and the domain structure of the corresponding translated protein products (lower half). Exons are indicated by boxes, and introns are shown as thin lines. Black shading of the exons indicates the open reading frame, whereas gray shading shows untranslated regions. Isoforms A, B, and C correspond to NM_004287.3, NM_054022, and NM_001014511.1, respectively. On the protein structures, the coiled-coil (CC), Q-SNARE (as indicated), and transmembrane (TM) domains are shown.

(D) A CLUSTALW alignment of orthologs of GOSR2 from multiple species. The orthologs were identified by using the homologene database, tblastn search of the NCBI nonredundant sequence database, and the SNARE database[24]. Species names and amino acid residue ranges are labeled on the left of the alignment. Identical residues are indicated by the gray background. Gly144 and the corresponding residue in other species are indicated by the black arrowhead; the glutamine residue from which the Q-SNARE gets its name is indicated by the white arrowhead. We performed alignments by using the EBI CLUSTALW server.[25]

periodic acid-Schiff histochemical stain or by electron microscopy of the cerebrum and cerebellum. The Golgi apparatus identified in lymphoid cells (Figure S1, available online) and anterior pituitary cells appeared normal.

We genotyped the subject, her unaffected brother, and her parents by using Affymetrix 250K Nsp SNP chips for the purpose of linkage mapping. Homozygosity mapping was performed as described previously[8] and identified a single region between rs3914090 and rs2240222 on chromosome 17 (chr17:36,483,334-46,021,780 bp; UCSC hg18 Genome Build) that achieved suggestive linkage attaining the maximum possible LOD score of 1.93 (Figure 1A).

We designed an on-array (Roche/Nimblegen) sequence-enrichment strategy for the chromosome 17 interval, totaling 3.29 Mbp of unique sequence. Probes on the array were based on the genomic coordinates from UCSC hg18 March 2006 genome build for Refseq genes, all human-expressed sequence tags (ESTs), and putative promoters, defined as 2 kb upstream of the first exon of a Refseq. Enriched DNA was sequenced on the Illumina GAIIx platform. We assembled reads to the hg18 build of the human genome by using Burrows-Wheeler Alignment tool and the Galaxy genome-analysis tool[9,10] with default parameters, except for *-d 5*, *-l 35*, and *-k 3*.[11] Eighty-eight

percent of bases tiled on the array were covered with at least ten 65 bp sequence reads (Figure 1A and Figure S2). Sequence variants were reported with SAMTools[12] and categorized with SeattleSeq. We identified 2055 sequence variants (Table S1) at a minimum of a 10-fold sequence coverage, in which the discrepant base accounted for at least 85% of the sequence reads (indicative of homozygous variants). Filtering based on dbSNP131 retained 121 unique variants (Table S1), and only four of these located to open reading frames (ORFs) or a splice site. Of the four variants, one was synonymous, and three were predicted to cause amino acid change: *KRT16* (MIM 148067), c.1223C>T, p.Thr408Met, (NM_005557.3); *COASY* (MIM 609855), c.1628G>A, p.Arg543His (NM_025233.5); and *GOSR2* (MIM: 604027), c.430G>T, p.Gly144Trp, (NM_004287.3) (Table S2). Sequencing a cohort of 73 unrelated individuals with unresolved PME revealed that five additional individuals from four families had the same homozygous *GOSR2* variant, c.430G>T, p.Gly144Trp, that was identified in case 1, (Figure 1B). No consanguinity was reported in their families. The c.430G>T *GOSR2* variant was not observed in 584 chromosomes from unaffected individuals or in dbSNP132. One of the four additional families was of German ancestry and the three others were of Dutch ancestry. Further analysis of one affected individual from each family with both microsatellite markers and Illumina 610 quad SNP chips revealed a founder haplotype that was most likely of European ancestry (Figure 1B and Table S3). All of the individuals tested with the SNP chips shared the same minimal haplotype (104 SNPs, spanning 0.3 cM) (Table S3). The two other missense variants identified in case 1 are located outside of this minimal haplotype; therefore, we focused further studies on the *GOSR2* c.430G>T, p.Gly144Trp, mutation as the most likely cause of PME in these families.

*GOSR2* is a member of the Qb-SNARE family of vesicle docking proteins.[13,14] There are three known alternatively spliced isoforms of *GOSR2* (A, B, and C), (Figure 1C), and all are predicted to be affected by the c.430G>T, p.Gly144Trp mutation. The glycine 144 residue (G144) is within the Qb-SNARE domain and shows remarkable conservation from mammals through to yeast[13] (Figure 1D). Moreover, this position is occupied by either a glycine or a similarly sized alanine residue within all human Qb-SNARE proteins.[14] Initially, we examined the possibility that the p.Gly144Trp substitution might affect GOSR2 protein stability; however, this was not altered (Figure S3). Interaction of the mutant GOSR2 with ARF1 measured by the split ubiquitin yeast two-hybrid method[15] was also not affected (Figure S4). Mutation of the equivalent glycine residue to aspartate in similar Qb-SNARE proteins prevents interaction between SNARE domains.[13,16,17] We therefore investigated the subcellular localization of GOSR2 and a known *cis*-Golgi marker GOLGA2[18] by indirect immunofluorescent staining and confocal microscopy of a patient-derived, primary skin fibroblast cell line. This showed that the GOSR2 p.Gly144Trp mutant protein fails to localize to the *cis*-Golgi

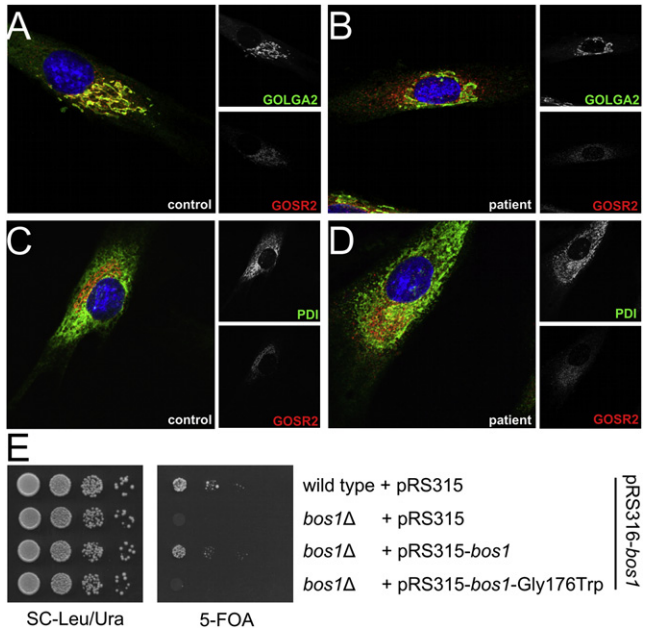


**Figure 2. GOSR2 Mutation, p.Gly144Trp, Functional Analysis**
(A–D) Example images taken by indirect immunofluorescent confocal microscopy of cultured primary human fibroblast cell lines derived from an unaffected female control (A and C) and case 1 (B and D). Cells were grown on glass coverslips, fixed with 4% paraformaldehyde, and then permeabilized with 0.2% saponin in phosphate buffered saline (PBS). The cells were then stained with an antibody specific to GOSR2 (mouse pAB, Abnova, Taipei City, Taiwan) (A–D; red channel) and costained with either the Golgi specific marker GOLGA2 (rabbit pAB, Abnova) (A and B) or the endoplasmic reticulum marker PDI (rabbit pAB, Santa Cruz Biotechnology, Santa Cruz, CA, USA) (C and D; green channel). Cells were embedded in Mowiol containing 4′, 6-diamidino-2-phenylindole (DAPI; blue channel) to stain nuclei and Dabco (Sigma Aldrich, Steinheim, Germany) as an antifading agent. Note that only the control cell line has evidence of costaining of GOLGA2 with GOSR2 (A; indicated by the yellow color). (E) Bos1 p.Gly176Trp cannot substitute bos1. Yeast strain BY4742 strain[26] was transformed with pRS316-*bos1* and the resulting strain transformed with *bos1* deletion cassettes constructed with PCR.[27] 5-fluoroorotic acid (5-FOA) is converted by Ura3 (present in pRS316-*bos1*) to 5-fluorouracil, which is toxic for the cell. We used negative selection with 5-FOA to confirm the *bos1* deletion (Δ*bos1*) strain. The pRS315-bos1 and pRS315-bos1-Gly176 vectors allow expression of the wild-type and mutant bos1 under negative selection conditions. Serial dilutions (1:10) of the indicated strains were spotted on SC-Leu/Ura and 5-FOA plates and incubated at 30°C for 48 hr. Only cells that lack a functional *bos1* gene after negative selection for the pRS316-*bos1* vector on the 5-FOA plates failed to thrive. Results indicate that cells transformed with pRS315-*bos1*-Gly176Trp are equivalent to the Δ*bos1* strain.

(Figures 2A–2D). The likely pathogenicity of the p.Gly144Trp mutation was investigated by constructing a yeast strain lacking the orthologous *bos1* (*Δbos1*) (see Tables S4 for plasmids Table S5 for yeast strains). The *Δbos1* strain failed to thrive and could not be rescued by the introduction of *bos1* carrying the orthologous (p.Gly176Trp) mutation (Figure 2E). This suggests that p.Gly144Trp is likely to be equivalent to a loss of function mutation.

The age of the c.430G>T, p.Gly144Trp mutation in *GOSR2* was estimated with a statistical model that

**Table 1. Comparison of Individuals with *GOSR2* (c.430G>T) Mutation**

| Case | Sex | Origin | Known Consanguinity | Age (Years) | First Symptoms | Other Seizures[a] | Motor | Cognition | Skeletal Abnormalities | EEG | CK (Normal < 170) |
|---|---|---|---|---|---|---|---|---|---|---|---|
| 1 | F | Australian | Yes | 32[b] | ataxia, age 2; tremor, age 7; absences, age 7–8; obvious myoclonus, age 8 | drop attacks, age 13; convulsive seizures, age 13 | areflexia, age 2; wheelchair, age 14; bedfast age, 22 | normal until ~age 25; mmemory difficulties later | scoliosis, pes cavus | generalized spike-wave, posterior emphasis photosensitive | 570–800 |
| 2 | F | German | No | 17 | ataxia, age 1–2; tremor, age 4; myoclonus, age 6 | drop attacks, age 14; myoclonic status | areflexia, age 2; wheelchair, age 15 | normal | scoliosis | generalized spike-wave, posterior emphasis photosensitive | 150–580 |
| 3 | F | Dutch | No | 32 | ataxia, age 3; myoclonus, age 6 | convulsive seizures, age 14 | areflexia, age 3; wheelchair, age 13 | normal | scoliosis, syndactly | generalized spike-wave photosensitive | 141–267 |
| 4 | F | Dutch | No | 30 | ataxia, age 2[c]; fine motor problems, age 5; worsening ataxia, age 7; absences, ~age 6; myoclonus, age 10 | tonic-clonic, age 12; drop attacks, age 14 | areflexia, age 7; wheelchair, age 24 | normal until ~ age 25; memory difficulties later | scoliosis, syndactly | generalized spike-wave, posterior emphasis photosensitive | 700–900 |
| 5a | F | Dutch | No | 24[b] | ataxia, age 2-3; myoclonus, age 6 | tonic-clonic seizures, age 21 | areflexia, age 6; wheelchair , age 14 | normal | scoliosis | generalized discharges photosensitive | 300–668 |
| 5b | M | Dutch | No | 28 | ataxia, age 2–3; myoclonus, age 5–6 | tonic-clonic seizures, age 24; absences; tonic seizures | areflexia, age 3; wheelchair, age 13 | normal | scoliosis | generalized discharges photosensitive | 174–213 |

[a] The distinction between true tonic-clonic seizures and myoclonic status could not be made in some cases.
[b] Deceased.
[c] Initially regarded as an acute ataxia, which improved.

describes the decay of haplotype sharing of the ancestral genomic segment due to recombination events over successive generations.[19] Common approaches to dating mutations that rely on mutant allele or haplotype frequencies[20] could not be applied to infer the age of the mutation because of the small sample size. The decay of haplotype sharing model states that the remaining ancestral segment length after $t$ generations has a gamma(2,$t$) distribution when the Haldane crossover model (no interference) is assumed. The model assumes neutral evolution, but the estimates can be shown to be unaffected by selection. We assumed that there was no selection because the disease is rare and recessive. A mutation age estimate was derived by taking a sample of $n$ ancestral segment lengths, $l_i$, estimated from cases 1–4 and 5b and then deriving a bias corrected maximum likelihood estimate (MLE) of the $t$ parameter in the model that is $t = (2n - 1) / (\sum l_i)$. Ancestral segment lengths were measured in Morgans and defined by regions where two or more affected individuals share identical homozygous SNPs flanking the c.430G>T mutation in *GOSR2* (Table S3). A small tract containing 23 heterozygous SNPs covering approximately 500 kb was observed in cases 3 and 4. We assumed that the ancestral segment extends beyond this point for another 136 markers where cases 1–4 share identical homozygous SNP genotypes (Table S3). A copy number variant (CNV) analysis of this heterozygous tract with PennCNV[21] did not detect a CNV (specifically a duplication), suggesting that the heterozygous tract in cases 3 and 4 might result from a double-recombination event. To derive the MLE, we plausibly assumed the ancestral segments in each affected individual were approximately the same age. We also assumed that the lengths were independent, which is equivalent to assuming the segments descend independently in the genealogy (a *star-shaped* genealogy). We obtained the exact confidence interval (CI) by deriving the sampling distribution of a pivotal quantity involving the estimate and the true mutation age by using known properties of the gamma distribution. In this case, the reported CI is only approximate because its derivation depends crucially on the independence assumption, and cases 3 and 4 share a comparatively recent ancestor based on their shared heterozygous marker tract that invalidates the independence assumption. We estimate the age of the mutation in *GOSR2* to be 181 generations with a 95% CI of (96, 343). Assuming a generation time of 20 years, this gives an age estimate of approximately 3,600 years.

The clinical histories of all six cases with the c.430G>T *GOSR2* mutation (Table 1) showed remarkable concordance; difficulty in walking was noticed in early childhood and was followed by the onset of action myoclonus around the age 6, sometimes associated with absence seizures. Tonic-clonic seizures were infrequent, but by their mid-teens five out of six subjects were wheelchair dependent because of sudden epileptic falls. Cognition was generally preserved, although there was some impairment in the third decade. All six cases had scoliosis, and two had syndactyly. EEGs showed an active generalized spike and wave and polyspike activity, often with a posterior predominance and with prominent photosensitivity (Figure S5). All cases had borderline or mildly elevated serum creatine kinase (CK); however, muscle histology and electromyography were normal, and the elevated CK was thought not to be explicable by muscle contractions due to seizures. MRI brain scans were normal except for mild cerebellar atrophy in one.

PMEs pose a significant challenge in accurate diagnosis because they are genetically heterogeneous and have relatively similar clinical presentations. The identification of mutations of *GOSR2* has helped to define a distinct form of PME that is distinguished by the early onset of ataxia by around age 2 and action myoclonus that develops around age 6. Unlike ULD, the course is relentlessly progressive and motor disability requires a wheelchair by the teens and further progression in the third decade. Scoliosis is not usually seen in PME; however, its presence in all six cases suggests it is part of the core phenotype. Other clinical clues could be syndactyly and a raised serum CK.

PMEs are remarkable for the relatively consistent clinical pattern of myoclonus, convulsive seizures, ataxia and generalized spike and wave discharges. Most of the gene products mutated in PMEs are known to be involved with posttranslational modification of proteins.[3] *GOSR2* is no exception; it has a role in protein transport from the endoplasmic reticulum and into the Golgi apparatus.[22] Furthermore, blocking the activity of *bos1* in yeast leads to a specific defect in posttranslational modification of glycophosphotidylinositol (GPI) anchored proteins.[23] Such molecular convergence suggests that certain neuronal groups might be particularly vulnerable to impaired posttranslational processing resulting in the characteristic phenotype of PME.

## Supplemental Data

Supplemental Data include five figures and five tables and can be found with this article online at http://www.cell.com/AJHG/.

## Acknowledgments

We are grateful for the cooperation of the families involved in this study. Thank you to Maike Langer, Thomas Hoefken, Lisa van Winsen, Maria Digenis, Bev Johns, and Rob King for excellent technical assistance; Paul Saftig for valuable advice; and Johannes Aerts for kindly providing us with the anti-human β-GC antibody 8E4. M.B. and J.G. were supported by the National Health and Medical Research Council (NH&MRC) with a Career Development Award and a Principal Research Fellowship, respectively. This project was supported by NH&MRC program grant 400121 and by the Research Training Group (GRK1459), funded by the Deutsche Forschungsgemeinschaft (DFG) to P.S. and M.S. The study was approved by the Austin Health Human Research Ethics Committee and informed consent was obtained from all participants.

Received: March 5, 2011
Revised: April 13, 2011
Accepted: April 14, 2011
Published online: May 5, 2011

## Web Resources

The URLs for data presented herein are as follows:

CLUSTALW at EBI, http://www.ebi.ac.uk/Tools/clustalw2/index.html
Galaxy, http://galaxy.psu.edu/
Homologene, http://www.ncbi.nlm.nih.gov/homologene/
Linkdatagen, http://bioinf.wehi.edu.au/software/linkdatagen/index.html
Online Mendelian Inheritance in Man (OMIM), http://www.omim.org
SeattleSeq, http://gvs.gs.washington.edu/SeattleSeqAnnotation/
SNARE Database, http://bioinformatics.mpibpc.mpg.de/snare/
UCSC Genome Browser, http://genome.ucsc.edu/
UniSTS, http://www.ncbi.nlm.nih.gov/unists/

## References

1. Jalanko, A., and Braulke, T. (2009). Neuronal ceroid lipofuscinoses. Biochim. Biophys. Acta *1793*, 697–709.
2. Berkovic, S.F., Andermann, F., Carpenter, S., and Wolfe, L.S. (1986). Progressive myoclonus epilepsies: specific causes and diagnosis. N. Engl. J. Med. *315*, 296–305.
3. Ramachandran, N., Girard, J.M., Turnbull, J., and Minassian, B.A. (2009). The autosomal recessively inherited progressive myoclonus epilepsies and their genes. Epilepsia *50* (*Suppl 5*), 29–36.
4. Lehesjoki, A.E. (2003). Molecular background of progressive myoclonus epilepsy. EMBO J. *22*, 3473–3478.
5. Berkovic, S.F., Dibbens, L.M., Oshlack, A., Silver, J.D., Katerelos, M., Vears, D.F., Lüllmann-Rauch, R., Blanz, J., Zhang, K.W., Stankovich, J., et al. (2008). Array-based gene discovery with three unrelated subjects shows SCARB2/LIMP-2 deficiency causes myoclonus epilepsy and glomerulosclerosis. Am. J. Hum. Genet. *82*, 673–684.
6. Bassuk, A.G., Wallace, R.H., Buhr, A., Buller, A.R., Afawi, Z., Shimojo, M., Miyata, S., Chen, S., Gonzalez-Alegre, P., Griesbach, H.L., et al. (2008). A homozygous mutation in human PRICKLE1 causes an autosomal-recessive progressive myoclonus epilepsy-ataxia syndrome. Am. J. Hum. Genet. *83*, 572–581.
7. Dibbens, L.M., Michelucci, R., Gambardella, A., Andermann, F., Rubboli, G., Bayly, M.A., Joensuu, T., Vears, D.F., Franceschetti, S., Canafoglia, L., et al. (2009). SCARB2 mutations in progressive myoclonus epilepsy (PME) without renal failure. Ann. Neurol. *66*, 532–536.
8. Corbett, M.A., Bahlo, M., Jolly, L., Afawi, Z., Gardner, A.E., Oliver, K.L., Tan, S., Coffey, A., Mulley, J.C., Dibbens, L.M., et al. (2010). A focal epilepsy and intellectual disability syndrome is due to a mutation in TBC1D24. Am. J. Hum. Genet. *87*, 371–375.
9. Blankenberg, D., Von Kuster, G., Coraor, N., Ananda, G., Lazarus, R., Mangan, M., Nekrutenko, A., and Taylor, J. (2010). Galaxy: A Web-Based Genome Analysis Tool for Experimentalists. Curr Protoc Mol Biol, Chapter 19, Unit 19.10.1-21.
10. Goecks, J., Nekrutenko, A., and Taylor, J.; Galaxy Team. (2010). Galaxy: a comprehensive approach for supporting accessible, reproducible, and transparent computational research in the life sciences. Genome Biol. *11*, R86.
11. Li, H., and Durbin, R. (2009). Fast and accurate short read alignment with Burrows-Wheeler transform. Bioinformatics *25*, 1754–1760.
12. Li, H., Handsaker, B., Wysoker, A., Fennell, T., Ruan, J., Homer, N., Marth, G., Abecasis, G., and Durbin, R.; 1000 Genome Project Data Processing Subgroup. (2009). The Sequence Alignment/Map format and SAMtools. Bioinformatics *25*, 2078–2079.
13. Fasshauer, D., Sutton, R.B., Brunger, A.T., and Jahn, R. (1998). Conserved structural features of the synaptic fusion complex: SNARE proteins reclassified as Q- and R-SNAREs. Proc. Natl. Acad. Sci. USA *95*, 15781–15786.
14. Bock, J.B., Matern, H.T., Peden, A.A., and Scheller, R.H. (2001). A genomic perspective on membrane compartment organization. Nature *409*, 839–841.
15. Sikorski, R.S., and Hieter, P. (1989). A system of shuttle vectors and yeast host strains designed for efficient manipulation of DNA in Saccharomyces cerevisiae. Genetics *122*, 19–27.
16. Fasshauer, D., Bruns, D., Shen, B., Jahn, R., and Brünger, A.T. (1997). A structural change occurs upon binding of syntaxin to SNAP-25. J. Biol. Chem. *272*, 4582–4590.
17. Brennwald, P., Kearns, B., Champion, K., Keränen, S., Bankaitis, V., and Novick, P. (1994). Sec9 is a SNAP-25-like component of a yeast SNARE complex that may be the effector of Sec4 function in exocytosis. Cell *79*, 245–258.
18. Nakamura, N., Rabouille, C., Watson, R., Nilsson, T., Hui, N., Slusarewicz, P., Kreis, T.E., and Warren, G. (1995). Characterization of a cis-Golgi matrix protein, GM130. J. Cell Biol. *131*, 1715–1726.
19. McPeek, M.S., and Strahs, A. (1999). Assessment of linkage disequilibrium by the decay of haplotype sharing, with application to fine-scale genetic mapping. Am. J. Hum. Genet. *65*, 858–875.
20. Slatkin, M., and Rannala, B. (2000). Estimating allele age. Annu. Rev. Genomics Hum. Genet. *1*, 225–249.
21. Wang, K., Li, M., Hadley, D., Liu, R., Glessner, J., Grant, S.F.A., Hakonarson, H., and Bucan, M. (2007). PennCNV: an integrated hidden Markov model designed for high-resolution copy number variation detection in whole-genome SNP genotyping data. Genome Res. *17*, 1665–1674.
22. Hay, J.C., Klumperman, J., Oorschot, V., Steegmaier, M., Kuo, C.S., and Scheller, R.H. (1998). Localization, dynamics, and protein interactions reveal distinct roles for ER and Golgi SNAREs. J. Cell Biol. *141*, 1489–1502.
23. Morsomme, P., Prescianotto-Baschong, C., and Riezman, H. (2003). The ER v-SNAREs are required for GPI-anchored protein sorting from other secretory proteins upon exit from the ER. J. Cell Biol. *162*, 403–412.
24. Kloepper, T.H., Kienle, C.N., and Fasshauer, D. (2007). An elaborate classification of SNARE proteins sheds light on the conservation of the eukaryotic endomembrane system. Mol. Biol. Cell *18*, 3463–3471.
25. Thompson, J.D., Higgins, D.G., and Gibson, T.J. (1994). CLUSTAL W: improving the sensitivity of progressive multiple sequence alignment through sequence weighting, position-specific gap penalties and weight matrix choice. Nucleic Acids Res. *22*, 4673–4680.

26. Winzeler, E.A., Shoemaker, D.D., Astromoff, A., Liang, H., Anderson, K., Andre, B., Bangham, R., Benito, R., Boeke, J.D., Bussey, H., et al. (1999). Functional characterization of the S. cerevisiae genome by gene deletion and parallel analysis. Science *285*, 901–906.

27. Longtine, M.S., McKenzie, A., 3rd, Demarini, D.J., Shah, N.G., Wach, A., Brachat, A., Philippsen, P., and Pringle, J.R. (1998). Additional modules for versatile and economical PCR-based gene deletion and modification in Saccharomyces cerevisiae. Yeast *14*, 953–961.